

Self-pulsing discharges in pre-heated air at atmospheric pressure

Mário Janda¹, Zdenko Machala¹, Lukáš Dvonč¹, Deanna Lacoste² and Christophe O Laux²

¹ Division of Environmental Physics, Faculty of Mathematics, Physics and Informatics, Comenius University, Mlynska dolina F2, 84248 Bratislava, Slovakia

² Laboratoire EM2C, CNRS UPR 288, École Centrale Paris, Châtenay-Malabry, 92295 Cedex, France

E-mail: janda@fmph.uniba.sk

Received 31 July 2014, revised 4 November 2014

Accepted for publication 17 November 2014

Published 17 December 2014



CrossMark

Abstract

The paper presents investigations of self-pulsing discharges in atmospheric pressure air pre-heated to 300–1000 K. Despite using a direct-current power supply, two self-pulsing discharge regimes, a repetitive transient spark (TS) and a repetitive streamer (RS) were generated. The pulse repetition frequency, on the order of a few kHz, can be controlled by adjusting the generator voltage. The TS is a discharge initiated by a streamer, followed by a short (tens of ns) spark current pulse (~ 1 A), associated with the total discharging of the internal capacity of the electric circuit. The TS is suitable for the study of ‘memory’ effects (pre-heating, pre-ionization) on the mechanisms of streamer-to-spark transition and electrical breakdown in atmospheric pressure air. The TS regime was stable below ~ 600 K. Above ~ 600 K, a stable repetitive streamer (RS) regime was observed. In this regime, the breakdown and spark did not occur. After the initial streamer, the internal capacity of the electrical circuit discharged partially. With further pre-heating of the gas, the stable TS appeared again at ~ 1000 K.

Keywords: self-pulsing discharges, transient spark, breakdown mechanism

(Some figures may appear in colour only in the online journal)

1. Introduction

Many applications of atmospheric pressure non-equilibrium ‘cold’ plasmas were studied during the last few decades [1–4]. Cold plasmas can be generated by various electrical discharges [5–8], where the energy is selectively delivered to free electrons. The accelerated ‘hot’ electrons are able to initiate various chemical reactions, while the temperature of the gas does not change significantly.

Several techniques were developed to prevent transition of the reactive ‘cold’ plasma to the thermal plasma. Three of the most common ways are based on (1) covering at least one electrode by an insulator (e.g. dielectric barrier discharge [9–11]), (2) using very short high voltage (HV) pulses [12–17], or (3) ballasting the direct-current (dc) discharge with a current-limiting resistor. We will only discuss the third approach, which is relevant to the discharges described in this paper.

The combination of a dc power supply and a large ballast resistor ($R > 1$ M Ω) is probably the simplest and most

cost-efficient way to generate a non-thermal plasma at atmospheric pressure between two metallic electrodes. The transition to arc is avoided since the ballast resistor limits the discharge current to a few mA. Several types of discharges can be generated this way, depending on the gas composition, flow rate, value of R and electrode geometry [18–23]. Beside a pulseless dc glow discharge (GD) [21, 22, 24], often mistakenly considered as an arc, there are also pulsed discharges: the prevented spark introduced by [18, 25–27] and its more general case the transient spark (TS) [28–30].

The transient spark is a filamentary discharge initiated by a streamer, followed by a short (~ 10 – 100 ns) high current (~ 1 – 10 A) pulse. Transition to a typical arc or a spark discharge is inhibited by the large external resistor R (5– 10 M Ω), as well as by the small internal capacity C (10– 40 pF) of the circuit. The process of periodical charging and discharging of C repeats with a characteristic frequency of a few kHz that can be controlled by changing the generator dc voltage.

Thanks to the short duration of the current pulse, the plasma generated by the TS has different properties than the plasma generated by an ordinary spark, with some $\sim 100 \mu\text{s}$ or ms long pulses. Like the spark, the TS pulses generate a highly reactive plasma with excited atomic radicals (O^* , N^*), excited molecules N_2^* and ions N_2^{+*} , but the gas temperature T is much lower than the vibrational temperature T_v of $\text{N}_2(\text{C})$, confirming the non-equilibrium character of the TS as opposed to the spark. Furthermore, the power of the TS is also relatively low in comparison with an ordinary spark. The energy discharged in one TS pulse is around 0.1–1 mJ.

The TS total power input increases with repetition frequency f from about 0.1 to 2 W [19, 28]. The increase of f is also accompanied by a heating of the gas up to $\sim 550 \text{ K}$ in the generated plasma channel [30]. For this reason, TS is not applicable where elevated temperatures can be harmful, e.g. for the treatment of heat sensitive solid materials, but is applicable for flue gas cleaning [19] or bio-decontamination [31] and has potential for stabilizing lean flames [32]. In the latter application, the treated gas itself can be hot and the additional heating of a small gas volume between the electrodes may not be significant.

The elevated temperature of the background gas can have a significant influence on the properties of the TS discharge. First, there is a decrease of the gas density N at elevated gas temperature. This leads to changes of discharge properties similar to those achievable by lowering the pressure at constant temperature. Second, the increase of temperature influences the rate coefficients of many chemical reactions. At higher temperature, we expect faster thermal detachment of electrons from negative ions and slower attachment and recombination reactions of electrons [33–35].

However, decreasing the pressure or increasing the temperature are not equivalent, as shown in [36]. This can be demonstrated by showing the differences between a glow discharge at ambient temperature and low pressure and a glow discharge at atmospheric pressure and elevated temperature. At low pressures, the GD has a diffuse character and its positive column can be extended quite easily [6]. On the other hand, at atmospheric pressure and elevated temperature, the GD has a more filamentary structure and its scaling is more difficult. In [20], multiple electrode configurations or thermionic cathodes and tubes with swirl gas flow had to be used to obtain larger plasma volumes.

Pai *et al* [37] showed that increasing the initial ambient gas temperature T^i also has a significant influence on the characteristics of nanosecond repetitively pulsed (NRP) discharges. Three different regimes were observed, among them a ‘spark’ regime with visual and electrical characteristics similar to those of the TS. The effect of an elevated temperature on a similar NRP discharge was also observed by Yin and Adamovich [38]. The pre-heating substantially reduced discharge filamentation and allowed sustaining a stable, diffuse and uniform non-equilibrium plasma.

Changes of TS properties were also observed even when operating the discharge in a gas at initial temperature $T^i = 300 \text{ K}$ [30]. With increasing TS repetition frequency f , the accompanying heating of the gas caused the current pulses

to become smaller and broader. A decrease of the breakdown voltage and shortening of the streamer-to-spark transition time was also observed at higher f . However, from the study of TS at $T^i = 300 \text{ K}$, we cannot definitely conclude that these changes are solely caused by pre-heating, because we are not able to separate the influence of the pre-heating from other effects, such as the accumulation of metastable species, or the increase of the pre-ionization level. Thus, to resolve this problem, we studied TS in atmospheric pressure air externally pre-heated up to 1000 K. The results are presented in this paper.

Since the TS is a discharge operating on the streamer-to-spark transition, this study is also interesting for the understanding of streamer breakdown in atmospheric pressure air. Electrical breakdown is a crucial issue for the generation of electrical discharges, as well as for the design of high voltage (HV) devices. The first studies of this phenomenon already appeared several decades ago [39–41]. However, because of the complexity of this problem, investigations of the breakdown mechanism, streamers and their propagation still continue [42–50]. The TS in pre-heated air thus enables us to study the role of the initial gas temperature and the influence of the repetition frequency on the streamer-to-spark transition and on electrical breakdown in atmospheric pressure air at voltages near the breakdown threshold.

In this paper we will present a study of the various discharge regimes observed in pre-heated air (300–1000 K), in the configuration used to generate the TS discharge. Section 2 describes the experimental setup and section 3 describes computational method used for kinetic modeling. Section 4 presents the results obtained and a discussion of the observed discharge regimes. The possible role of a ‘memory’ effect on the electrical breakdown is also discussed.

2. Experimental setup

The experimental set-up is depicted in figure 1. All experiments were carried out in atmospheric pressure air preheated to 300–1000 K with a controlled resistive heater. The velocity of the air flow was about $2 \text{ m}\cdot\text{s}^{-1}$, parallel to the inter-electrode axis. The distance between the steel electrodes (point-to-point configuration with anode at the top) was 5 mm. The electrodes were made of a 2 mm diameter rod. The anode tip was sharpened whereas the cathode was blunt. The radius of curvature of the anode tip was of the order of $100 \mu\text{m}$. We re-sharpened the anode tip manually as needed whenever it became worn. The radius of curvature of the cathode was of the order of a millimeter. The larger radius of the cathode had to mimic the point-to-plane configuration of electrodes used in our previous research of TS [29, 30], since it was not possible to use the point-to-plane geometry in this setup with preheated airflow.

A high voltage (HV) positive polarity dc power supply HCL 14–20 000 placed in series with a resistor ($R = 10 \text{ M}\Omega$) was used to generate the discharge. An additional small resistor $r = 1 \text{ k}\Omega$ was inserted between the anode and the cable connected to the resistor R (see figure 1). The role of r was to eliminate the oscillations of electric signals caused by the

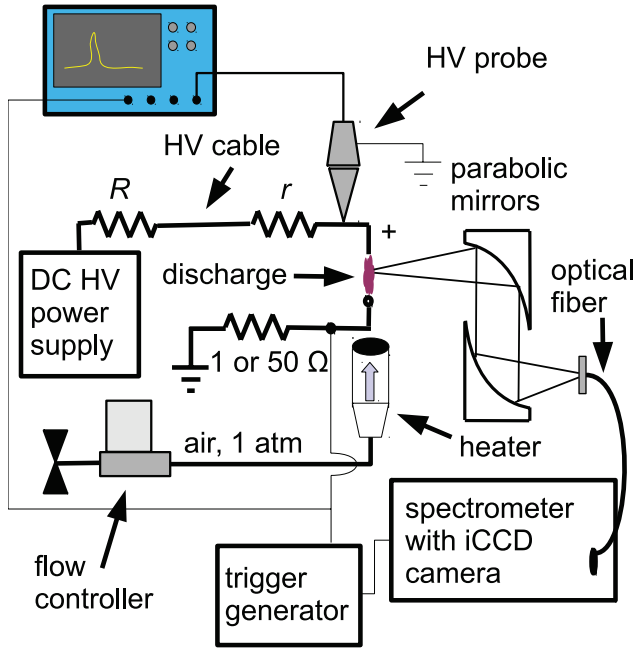


Figure 1. Schematic of the experimental set-up.

internal inductances of the HV cable and of the grounding wire. The discharge voltage was measured by a HV probe LeCroy PMK-14kVAC and the discharge current was measured on a $50\ \Omega$ or $1\ \Omega$ resistor shunt. Voltage and current signals were recorded by a 350 MHz digitizing oscilloscope LeCroy Waverunner 434 (maximum $2\ \text{GS}\cdot\text{s}^{-1}$).

Time-resolved emission UV-visible spectra were obtained using a spectrometer (Acton SpectraPro 2500i) fitted with an intensified charge-coupled device (iCCD) camera (Princeton Instruments PI-MAX). The iCCD camera was triggered by a TTL generator. This generator was triggered directly by the current signal, causing a delay of less than 10 ns. This delay, in addition to the delay caused by the coaxial cables, was partially compensated by using a 2 m long optical fiber. However, an additional delay was introduced by the iCCD camera itself, so we were not able to measure spectra during the first 70 ns following the rising edge of the synchronizing current pulse.

We used the spectra of the $\text{N}_2(\text{C}^3\Pi_u-\text{B}^3\Pi_g)$ 2nd positive system to determine the gas temperature T , since it can be well approximated by the rotational temperature of excited $\text{N}_2(\text{C}^3\Pi_u)$ species in the atmospheric air pulsed discharges [51]. This rotational temperature was inferred from the spectra using SPECAIR [52]. The iCCD camera was synchronized with the beginning of the streamer pulse—by the current signal measured on $50\ \Omega$ shunt. The collection of light was made by a pair of parabolic mirrors focused on a small area ($50\ \mu\text{m}$ in diameter) below the tip of the anode.

3. Kinetic model

Modeling of chemical kinetics is an effective tool for the description of complex systems [53, 54]. Chemical kinetics can be used to determine the density evolution of species, which are not measurable via available analytic and

experimental techniques. In order to develop a valid plasma kinetic model, it is necessary to generate a set of differential equations of the 1st order describing the density evolutions (N_i) of all important species generated in the plasma:

$$\frac{dN_i}{dt} = \sum_j S_{ij}. \quad (1)$$

Here, S_{ij} is a production term for species X_i via a specific reaction j . The rate coefficients of reactions in the plasma must be described by at least two different temperatures. The temperature of electrons characterizes the rates of electron impact reactions, whereas the temperature of neutral species defines the rate coefficients of all other reactions. The temperature of electrons can be calculated as a function of gas composition and reduced electric field strength (E/N) by solving the Boltzmann equation.

We based our model on existing ZDPlasKin libraries [55]. ZDPlasKin includes a DVODE solver for the numerical solution of a system of ordinary differential equations. The authors of ZDPlasKin also provide a ready-to-use list of plasmachemical processes in nitrogen-oxygen mixtures, also used in [56]. It is based mainly on Capitelli *et al* [35]. The ZDplasKin package also includes a Bolsig + package to solve the Boltzmann equation. The required electron scattering cross sections were taken from [57, 58]. We added a module compatible with ZDPlasKin to describe the evolutions of E/N , T and total density of neutrals N corresponding to the conditions of our discharges.

4. Results and discussion

A pulse-less DC glow discharge (GD) might be considered as the natural type of discharge achievable in our setup, since we are using a DC power supply. However, the GD is sustained due to energy released by an electric current and the specific energy deposition must exceed a critical value [24]. As a result, there exists a threshold current $I_{\text{min}}^{\text{GD}}$ for an establishment of a stable GD. Thus, when the generator voltage V_g applied to the stressed electrode is progressively increased, we first observe a streamer corona. Further increase of V_g leads to the onset of self-pulsing discharges. We observed two types of self-pulsing discharges under the studied conditions, the transient spark (TS) mentioned in introduction and the repetitive streamer (RS) discharge that occurs at higher T^i and will be described in section 4.2.

The increase of V_g is accompanied by an increase of the mean current I_{mean} of these self-pulsing discharges. The GD can be obtained only when I_{mean} exceeds a certain minimum value ($I_{\text{min}}^{\text{GD}}$). In practice, the stability of the GD depends on more parameters. Instability of the GD and appearance of other discharge regimes, such as transient spark or ultra-corona can be also achieved by an increased gas flow [23].

We are focusing on the self-pulsing discharges in this paper, but we stress out that the GD regime is also important, since $I_{\text{min}}^{\text{GD}}$ imposes an upper limit of existence these self-pulsing discharges. Figure 2 shows a simplified ‘map’ of the discharge regimes observed in our setup as a function

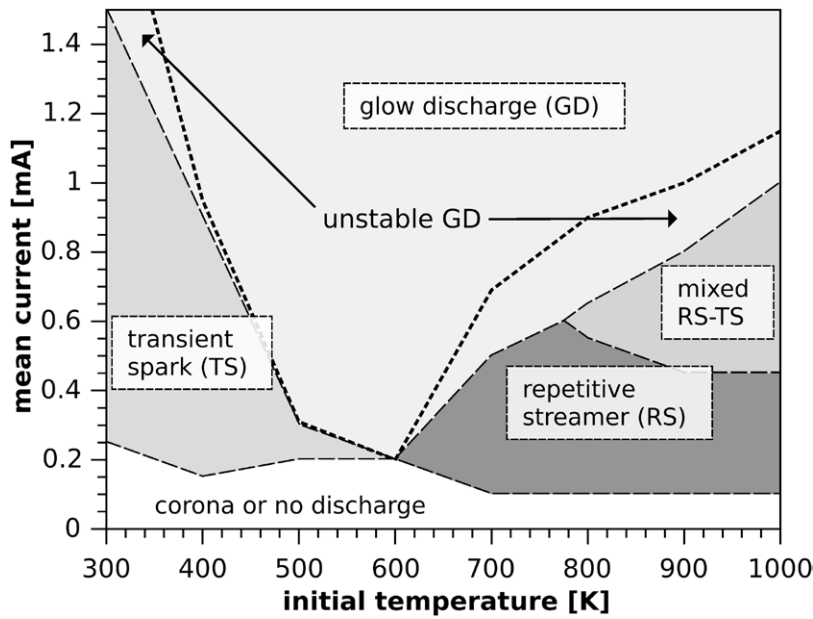


Figure 2. Discharge regimes depending on the mean discharge current and the initial gas temperature T^i , air flow velocity $2 \text{ m}\cdot\text{s}^{-1}$, gap distance 5 mm , $R = 10 \text{ M}\Omega$.

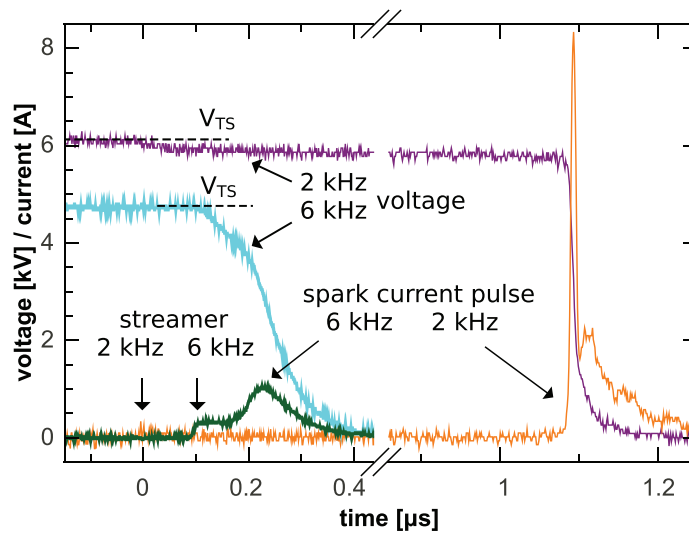


Figure 3. Typical voltage and current waveforms of the transient spark at ‘low (2 kHz)’ and ‘high’ (6 kHz) frequency. For clarity, the waveform of TS at 6 kHz was omitted on the right side from the x -axis break.

of the mean discharge current and the initial gas temperature T^i . The boundaries between these discharges are not very distinct. There are regions where two or three unstable discharge regimes co-exist. For example, when the RS repetition frequency exceeded $\sim 6 \text{ kHz}$, irregular TS current pulses were observed above $\sim 750 \text{ K}$ mixed with the RS discharge pulses. The stable TS was observed only below 600 K and then again at 1000 K . Both self-pulsing discharges (TS and RS) will be discussed in the next sections.

4.1. Transient spark for T^i below 600 K

Transient spark (TS) is a discharge of a repetitive streamer-to-spark transition type. TS is initiated by a streamer creating

a relatively conductive plasma bridge between the electrodes. This streamer appears when the potential on the stressed electrode reaches voltage V_{TS} , characteristic of the TS. After a certain delay (streamer-to-spark transition time τ), the streamer phase is followed by a spark phase. During this phase (time $1.1 \mu\text{s}$ in figure 3), the voltage V on the HV electrode drops to almost zero (figure 3) and the current reaches a high value ($\sim 1\text{--}10 \text{ A}$).

After the internal capacity C of the circuit is completely discharged (i.e. after the end of the transient spark current pulse), the potential V on the stressed electrode gradually increases as the plasma conductivity decreases and C recharges. A new TS pulse, initiated by a new streamer, occurs when V reaches again the breakdown voltage V_{TS} .

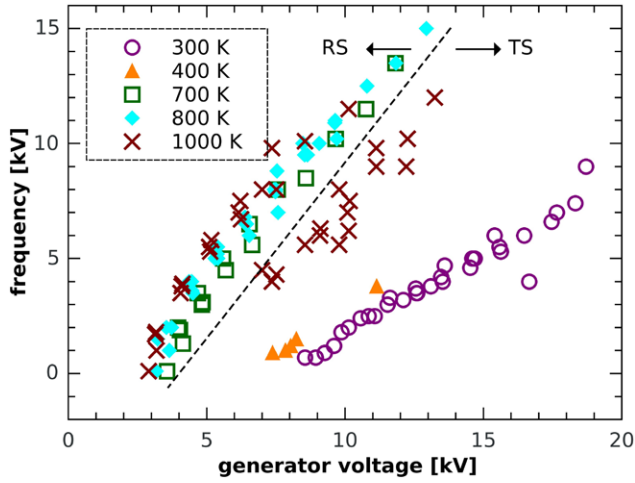


Figure 4. Repetition frequency of RS and TS discharge regimes as a function of generator voltage at various initial temperatures.

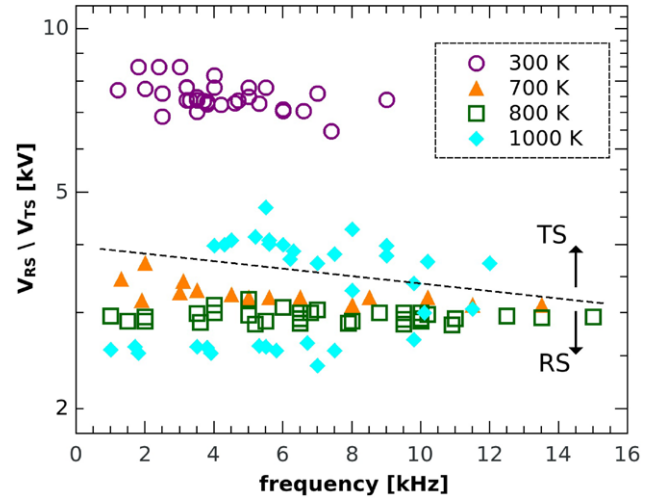


Figure 6. Maximum discharge voltage of RS and TS discharge regimes as a function of repetition frequency for various initial temperatures.

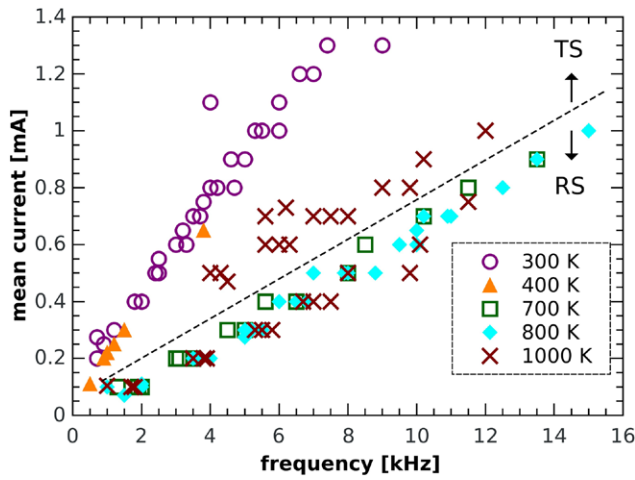


Figure 5. Mean discharge current as a function of the repetition frequency at various initial temperatures.

The TS is thus based on repetitive charging and discharging of C . The repetition frequency f of this process can be controlled by the generator voltage V_g [29]:

$$f = \frac{1}{RC \ln \left[\frac{V_g}{V_g - V_{TS}} \right]} \quad (2)$$

The increase of V_g leads to an increase of f (figure 4), but also to an increase of I_{mean} (figure 5). When I_{mean} approaches $I_{\text{min}}^{\text{GD}}$, the transition to GD occurs. At $T^i = 300$ K, $I_{\text{min}}^{\text{GD}} \approx 2$ mA. A stable TS regime is typically observed only if $I_{\text{mean}} \lesssim 1.5$ mA. If I_{mean} is approximately between 1.5–2 mA, an unstable regime with alternating GD and TS discharges appears [29].

A similar behavior of TS, i.e. the increase of I_{mean} and f with increasing V_g , was also observed at $T^i = 400$ K and 500 K. However, the highest TS frequency was in these cases limited by the $I_{\text{min}}^{\text{GD}}$ that decreases with increasing T^i below 600 K (figure 2). The transition to (unstable) GD thus occurred at lower I_{mean} and f . At $T^i = 600$ K, no stable TS

discharge was observed at all. The $I_{\text{min}}^{\text{GD}}$ increases at higher initial temperatures, but a stable TS regime was observed again at $T^i = 1000$ K. This ‘high temperature TS regime’ is discussed in subsection 4.3.

Above $T^i = 600$ K, the repetitive streamer (RS) discharge discussed in section 4.2 was observed. In the RS, streamers are followed by only partial discharging of C and partial voltage drop. This is its major difference compared to the TS discharge, where streamers initiate breakdown and spark formation. The breakdown mechanism in the TS at $T^i < 600$ K is discussed in the next subsection.

4.1.1. Breakdown mechanism in the transient spark. The discharge current after the streamer decreases (figure 3) and the plasma is in the decay phase with the electron density decreasing. Several mechanisms can revert the decrease of the current after the streamer and initiate the breakdown: chemical or stepwise ionization [43, 47, 59], gas density decrease due to heating and hydrodynamic expansion of the plasma channel [60–62], channel contraction [59, 63], or attachment control processes [64–66].

In the TS, several processes may influence the breakdown mechanism and their relative roles can change with f . The breakdown is influenced by a ‘memory’ effect at higher frequencies due to pre-heating and accumulation of various species created by previous TS pulses. The breakdown voltage V_{TS} decreases (figure 6) due to the pre-heating of the gas between the electrodes (from 300 K up to ~ 550 K at ~ 10 kHz). The average streamer-to-spark transition time τ shortens significantly with increasing f from a few μs down to ~ 100 ns [30]. At $f \approx 6$ kHz, there was almost no time delay between the streamer and the spark phases. We even observed almost direct transition from streamer to spark without a decrease of the current in between (figure 7). In generally, the current decrease slows down with increasing f .

We used kinetic modeling to explain this phenomenon, by calculating the evolution of the electron density after the streamer at different temperatures. The temperature was kept

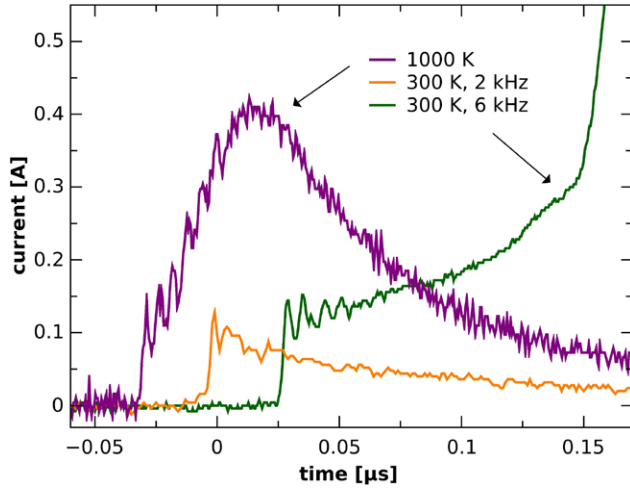


Figure 7. Typical current pulse of the transient spark at $T^i = 1000$ K, comparison with TS at $T^i = 300$ K, $f = 2$ kHz (only streamer phase shown here, excessive current spark phase will follow after a delay time of ~ 1 μ s) and $f = 6$ kHz. Initial time shifts of these 3 pulses are only shown for clarity.

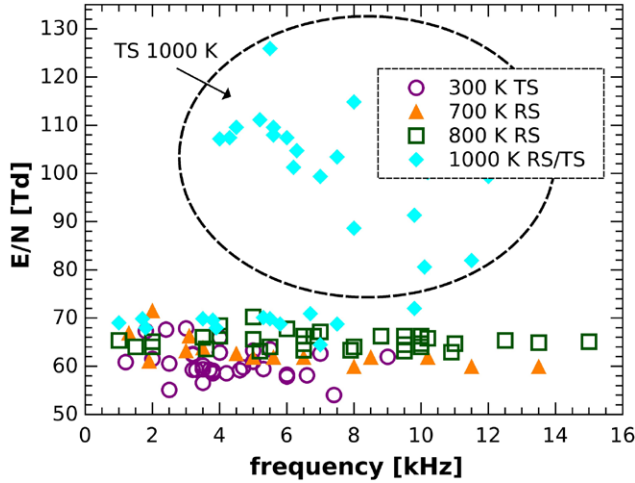


Figure 8. Estimated average reduced electric field in the plasma channel right after its establishment by a streamer.

constant during each simulation. The time evolution of E/N was modeled by a function

$$E/N(t) = E/N_{bg} + \alpha \times \exp\left\{-\frac{(t-t_s)^2}{2\sigma^2}\right\}, \quad (3)$$

where $\sigma = 2$ ns and $t_s = 30$ ns, and the E/N_{bg} is the reduced field established in the plasma after the streamer, assuming uniform axial distribution of the E/N . The streamer is simulated by the Gauss function (second term in (3)) with the center of the peak in time t_s . The total calculation time was 800 ns. The coefficient α was adjusted to achieve $n_e = 10^{14}$ cm^{-3} right after the streamer to be in agreement with experimental findings [67]. The initial density of electrons was chosen as 3×10^8 cm^{-3} . The density of all other species except N_2 and O_2 was set to zero.

The assumption of the uniform axial distribution of the E/N is just an approximation. The distribution of the attachment rate along the plasma filament produced by the primary streamer leads to the increase in the reduced electric field E/N

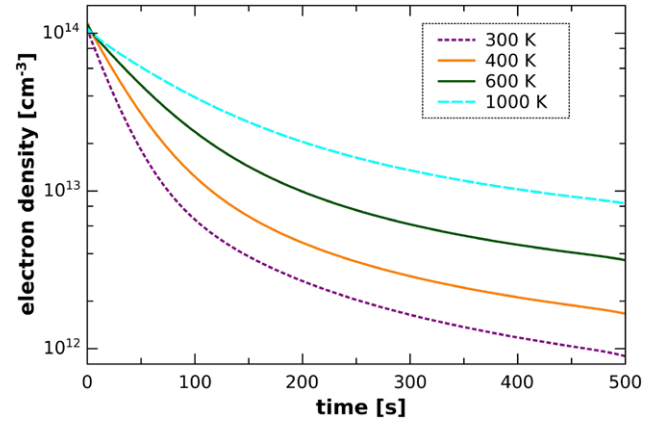
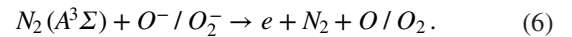
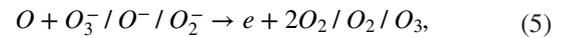
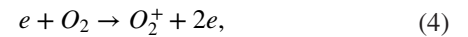


Figure 9. Calculated decrease of electron density after the streamer as a function of gas temperature.

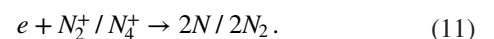
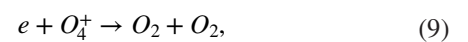
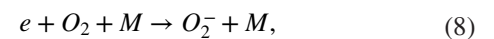
near the anode [64–66]. A decrease in gas density leads to the extension of this region which finally reaches the cathode, as was shown in the model of Bastien and Marode [65]. The propagation of this region with increased E/N was named the secondary streamer [68].

We estimated the average E/N in the plasma channel right after its establishment by a streamer to be ~ 60 – 70 Td (figure 8), with no significant dependence on f and T^i (except for the TS regime at $T^i = 1000$ K discussed in section 4.3). Typically, the E/N in the secondary streamer can be elevated to ~ 80 Td [66]. However, variation of E/N_{bg} in the range 60–80 Td had no significant influence on the evolution of n_e in our simulations. Even at 80 Td, the field is still not strong enough for direct electron-impact ionization processes to dominate. We therefore present here the results for $E/N_{bg} = 70$ Td only (figure 9).

Figure 9 shows that the decrease of the electron density slows down with the increasing temperature. The analysis of these calculations showed that the increase of temperature and decrease of N do not have very strong influence on the rate of electron production. Here is the list of the most important reactions:



More significant is the influence of increasing T on the electron loss processes. The most important reactions causing the decrease of the electron density at 300 K are:



Mainly reactions (8) and (9) depend strongly on T_g . At 600 K, the recombination of electrons with O_4^+ ions is already very weak. At 1000 K, the three-body attachment (equation (8)) slows down due to the decrease of N and reaction (7) dominates completely. Altogether, the decrease of n_e after the streamer slows down with increasing T . This can partially explain slower decrease of current after the streamer at higher f , where the gas inside the discharge channel is pre-heated up to ~ 550 K.

We assume that other ‘memory’ effect, related to the accumulation of various species from previous TS pulses, can also significantly decrease rate of current and n_e decrease after the streamer at higher f . Based on the list of the most important processes we assume that atomic oxygen O could play the most important role. The accumulation of O species was also experimentally observed in NRP discharge at 10 kHz [69]. The atomic oxygen species are produced from molecular oxygen O_2 . Thus, the accumulation of O would not only accelerate electron detachment from negative ions (reaction (5)), it would also be accompanied by a decrease of the density of O_2 , i.e. it would decrease the rate of electron attachment processes. We were able to simulate this also by increasing the initial density of O species and decreasing the O_2 density in the kinetic model. However, this cannot be considered yet as evidence. We must measure O species experimentally to prove this hypothesis.

Altogether, these calculations show that the increase of the temperature accompanied by the suppression of electron loss processes does lead to the slower decrease of n_e after the streamer. On the other hand, increase of n_e and current, leading to the spark requires another explanation. We suppose that it is also necessary to accelerate the ionization processes by the increase of E/N . In the TS, the increase of E/N after the streamer can be achieved only by the decrease of N due to gas heating.

In the TS at $T^i = 300$ K, the temperature increases up to ~ 1000 K during the streamer-to-spark transition phase [30] within a few hundreds nanoseconds. The heating is so fast that the flux of neutrals away from the heated discharge channel is probably not sufficient to keep pressure at atmospheric level, as it is shown in simulation of Naidis [70]. We therefore assume that the breakdown mechanism in the TS is mainly based on the gas density decrease suggested by Marode [60], i.e. heating of the channel via Joule heating and the two-step heating mechanism investigated by Rusterholtz *et al* [51] \rightarrow increase of the pressure \rightarrow hydrodynamic expansion \rightarrow decrease of N in the core of the channel \rightarrow increase of $E/N \rightarrow$ acceleration of ionization processes.

At the TS frequencies below ~ 3 kHz, a constriction of the discharge channel consistent with the simulations of Naidis [70] was observed [30], supporting this assumption. However, it was shown that increase of n_e and breakdown in contracting discharges is possible even at relatively weak fields thanks to the stepwise ionization processes [59]. There is even a positive feedback for the production of excited species in the contracting discharges [59]. In special cases, e.g. in negative corona in N_2 , the breakdown without initiating streamer is possible resulting from the contraction of the discharge channel [63].

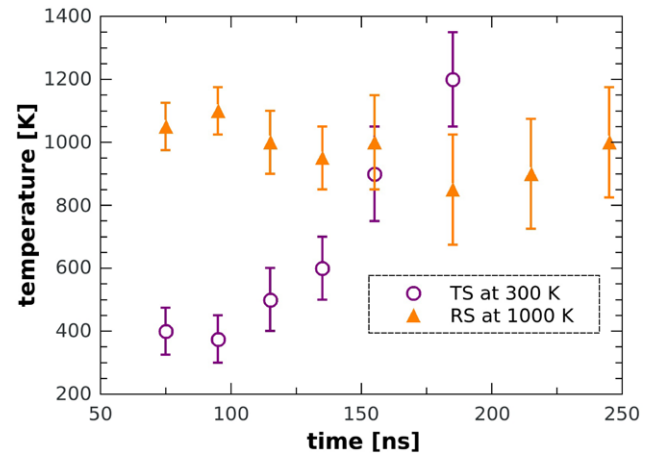


Figure 10. Time evolution of the gas temperature after the beginning of the streamer, TS at $T^i = 300$ K, $I_{\text{mean}} = 0.9$ mA, $f \approx 4$ kHz and the RS at $T^i = 1000$ K, $I_{\text{mean}} = 0.75$ mA, $f \approx 11$ kHz.

The secondary streamer was also observed in the evolution of the TS discharge [71]. Its role in the breakdown mechanism in TS has to be yet elucidated. The secondary streamer might play a significant role in fast heating in the TS during the streamer-to-spark transition phase. Even if electrons in the secondary streamer have not enough energy to ionize at $E/N = 80$ Td, they are able to generate excited N_2 crucial for the two-step fast heating mechanism investigated by Rusterholtz *et al* [51]. Moreover, excited N_2 species can be important for the stepwise ionization processes, too [59]. Further research of the TS breakdown mechanism is needed to resolve these questions.

4.2. Repetitive streamer (RS) discharge

Both the TS and RS discharge regimes are initiated by a streamer. However, discharge development after the initializing streamer differs significantly in these two regimes. Unlike in TS, there is no spark and no gas heating inside the plasma channel after the streamer in the RS (figure 10). The discharging of C in RS is only partial and the voltage drops to a certain non-zero value V_{min} (figure 11). After discharging, the potential at the HV electrode increases again as C recharges, until it reaches the value V_{RS} necessary for a new streamer resulting in another partial discharging of C .

From this electrical point of view, the RS discharge is similar to TS. The RS repetition frequency is also on the order of several kHz and can be controlled by the generator voltage V_g (figure 4). This frequency can be approximately calculated using equation (2), corrected for V_{min} , with V_{TS} replaced by V_{RS} :

$$f = \frac{1}{RC \ln \left[\frac{V_g - V_{\text{min}}}{V_g - V_{\text{RS}}} \right]} \quad (12)$$

The shape of the RS current pulse (figure 12) can be approximated by a sum of two currents, the current from the partial discharging of C (I_C) and a streamer current I_{streamer} :

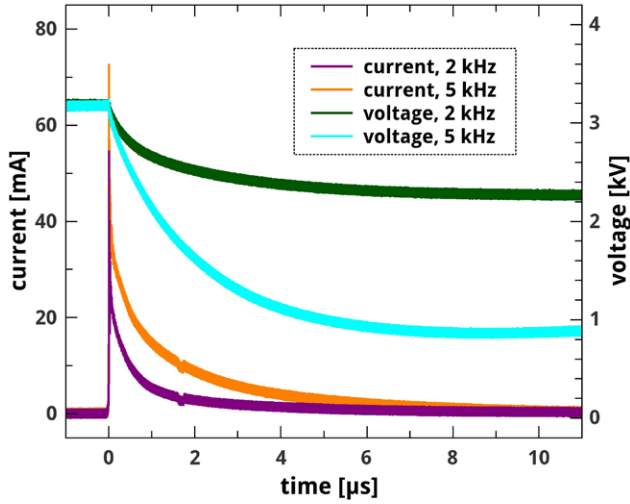


Figure 11. Typical RS current and voltage waveforms, $T^i = 700$ K, repetition frequencies 2 and 5 kHz.

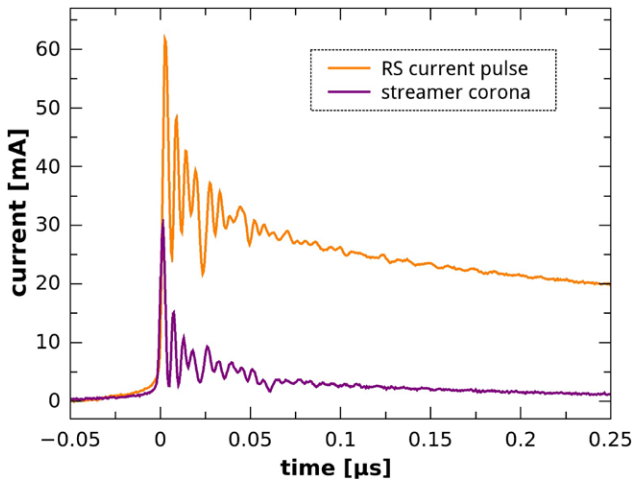


Figure 12. Comparison of RS current pulse ($f \approx 3$ kHz, $I_{\text{mean}} = 0.2$ mA, voltage drop $\Delta V \approx 1.7$ kV, $T^i = 700$ K) with an irregular streamer corona current pulse ($I_{\text{mean}} = 0.04$ mA, $\Delta V \approx 0$ kV, $T^i = 400$ K).

$$I(t) = I_{\text{streamer}} + I_C = I_{\text{streamer}} - C \times \frac{dV(t)}{dt}. \quad (13)$$

The relative contribution of these two currents changes with the f and T^i . Since V_{min} (figure 13) decreases and discharging time shortens (figure 14) with increasing f and T^i , the slope of the voltage decay and I_C are larger at high f and T^i . However, I_{max} of the RS (figure 15) is always much lower than I_{max} of the TS. The I_{max} of the RS is comparable with the peak current during the streamer phase of the TS (see figure 7).

4.2.1. Explanation of the RS discharge establishment. In the TS, local heating of the gas inside the thin plasma channel created by the streamer leads to its hydrodynamic expansion, decrease of N in the core of the plasma channel and breakdown. On the other hand, in the RS, the entire gas volume is preheated, N is lower already at the beginning of the streamer and the discharge has a slightly more diffuse character. The

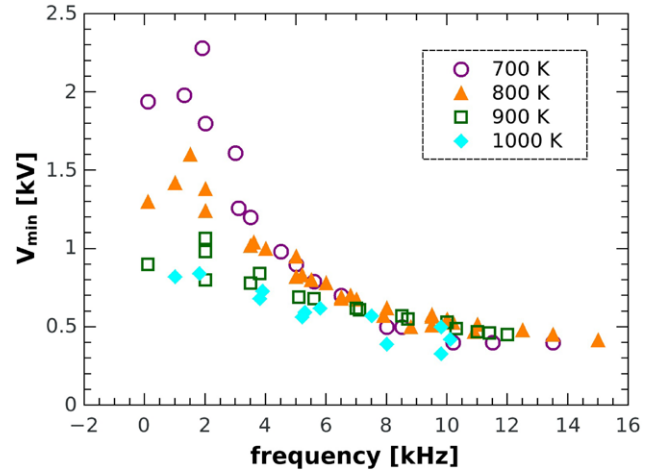


Figure 13. Minimum voltage in RS regime as a function of the repetition frequency and initial temperature.

volume density of the deposited energy per unit time after streamers is thus probably lower in the RS than in the TS discharge. Moreover, the radial energy flux away from the plasma channel should be higher in the RS due to lower N . This might be the reason why no increase of T after the RS streamer was observed (figure 10), while in the TS at $T^i = 300$ K we observed an increase of T after the streamer consistent with our previous observations [30]. The lack of fast heating after the streamer is the key factor why streamers do not initiate breakdown and the RS discharge regime is established.

The gas temperature evolution after the streamer was derived from the time resolved spectra of N_2 2nd positive system. Due to the short life time of $N_2(C^3\Pi_u)$, we were not able to follow the evolution of T for more than ~ 200 ns after the beginning of the streamer. We thus cannot exclude that gas heating continues later due to vibrational-translational (V-T) transfer. However, even if T increases up to ~ 1000 K a few μ s later, no breakdown would happen because V (and E) would have decreased too much by that time. The V_{min} is also reached in μ s time scale, as shown in figure 14. No fast gas heating in the plasma channel and a significant decrease of V after the streamer thus make the breakdown mechanism based on the hydrodynamic expansion impossible. This is supported by acoustic observation: in the RS, unlike in the TS, there was no hydrodynamic expansion noise audible in the RS discharge.

The relatively long continual decrease of V after the streamer in the RS can be explained by using our kinetic modeling. The decrease of n_e is slower at higher T (figure 9). This means that the conductivity of the plasma channel created by the streamer stays relatively high for a longer period. This enables a longer partial discharging of C and so the decrease of V after the streamer. This effect is also observable in the TS at $T^i = 300$ K and higher f (figure 3), where the gas inside the plasma channel is preheated to almost 600 K. However, unlike in the RS, the TS discharge channel at $T^i = 300$ K at higher f is very localized. The discharge repeatedly takes the same preheated thin gas channel, where accumulation of various species occurs. With increasing f , the rate of heating in the TS at $T^i = 300$ K does not slow down due to preheating and decrease of N inside the plasma channel. On the contrary, the memory

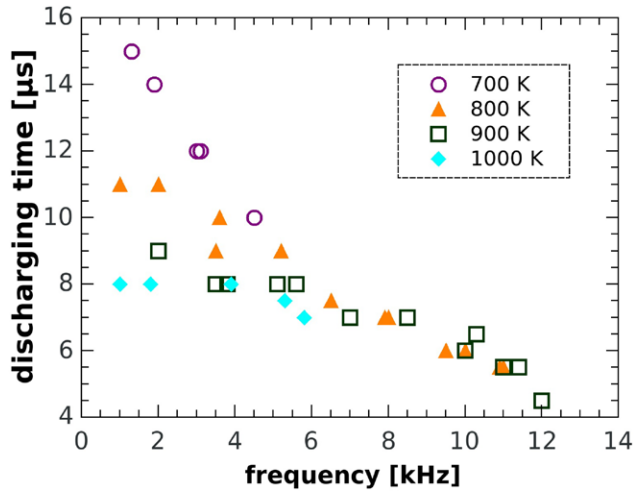


Figure 14. Duration of the discharging (delay between V_{RS} and V_{min}) as a function of the repetition frequency and initial temperature in the RS discharge.

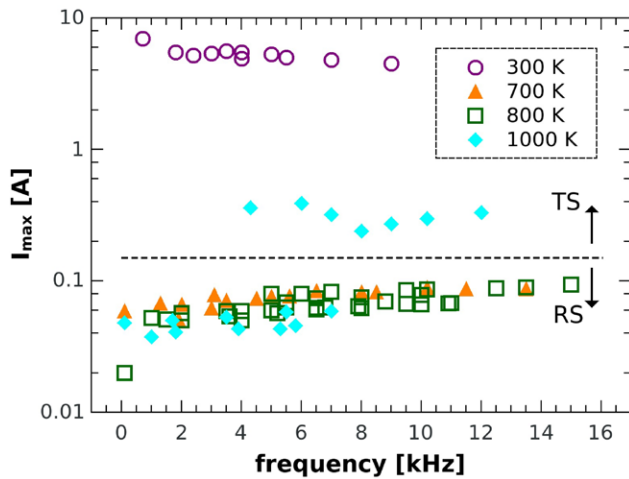


Figure 15. Peak current of RS and TS discharge regimes as a function of the repetition frequency at various initial temperatures.

effect accelerates the gas heating after the streamer and the breakdown occurs within ~ 100 ns, before V drops too much.

We assume that the memory effect influences also the RS above ~ 6 kHz. The V_{min} and discharging time in figures 13 and 14 are functions of both T^i and f only up to ~ 6 kHz. At higher frequencies, they only depend on f . The role of the memory effect could also play a certain role in the re-appearance of the breakdown and the TS regime at high f . It will be discussed in the next section.

4.3. Transient spark at $T^i = 1000$ K.

TS naturally occurred until $T^i = 600$ K and periods of unstable TS regime were re-observed at $T^i = 800$ – 900 K at high RS repetition frequencies. Stable TS discharge appeared again only at $T^i = 1000$ K. However, the TS pulses at $T^i = 1000$ K differ from those at $T^i = 300$ K (figure 7). There is no streamer-to-spark transition phase at $T^i = 1000$ K. The spark appears to occur immediately after the streamer.

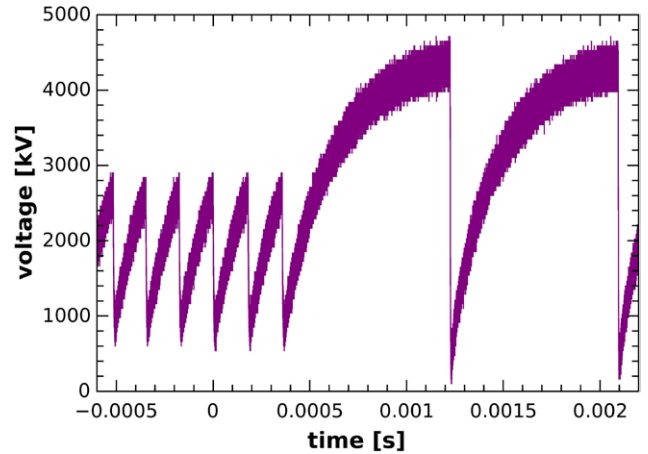


Figure 16. Voltage waveform showing transition from RS to TS discharge at $T^i = 1000$ K.

The analysis of voltage waveforms acquired at long time scale (figure 16) showed that there must be a different mechanism. After several RS pulses, no streamer appears when V on the needle electrode reaches V_{RS} . The streamer appears only after a longer period, when V reaches a higher value. After this streamer that develops at higher V , the estimated average E/N is also higher, probably above 110 Td (figure 8). This high E/N together with significantly suppressed attachment frequency at 1000 K can explain the immediate onset of the spark current after the streamer.

We cannot explain the disappearance of streamers at V_{RS} at a certain RS repetition frequency yet. However, the lowest f of stable TS was ~ 4 kHz (the frequency of the RS regime that could also be occasionally observed at the same V_g was above 6 kHz). We therefore suggest that it could also be related to a memory effect-pre-ionization. At 1000 K, the decrease of electron density is very slow (see figure 9). This could lead to the accumulation of a significant amount of charged species from previous RS pulses and the appearance of a space charge field. The increase of V at which streamers form indicates that conditions suitable for their formation are reached only when the external electric field becomes strong enough to overcome the influence of this space charge field.

5. Conclusions

The aim of our study was to investigate the behavior of self-pulsing discharges in atmospheric pressure air pre-heated to 300 – 1000 K. We generated two self-pulsing discharges, with relatively regular and controllable repetition frequency (on the order of kHz), named transient spark (TS) and repetitive streamer (RS).

The TS is a repetitive discharge of the streamer-to-spark transition type, initiated by a streamer, with the spark pulse duration and amplitude limited by the small amount of energy stored in the internal capacity of the circuit. A similar type of plasma, even at higher pulse repetition frequencies, can be generated using pulsed high voltage power supplies. The advantage of our approach is a simpler and cheaper electric setup using a DC high voltage power supply. This basic

research study of the TS in pre-heated air is important for its better understanding and further optimization for various applications, such as plasma assisted combustion.

We obtained stable TS only for initial air temperatures below 600 K and then again at 1000 K. The influence of pre-heating led to the establishment of another self-pulsing discharge regime named the repetitive streamer at initial gas temperatures above 600 K. In the RS, the breakdown to spark is suppressed and only a partial discharging of C after the initializing streamer occurs. With the TS we can deliver more power to the gas than with the RS regime. Thus, the re-establishment of the stable TS regime at ~ 1000 K is important for the application on lean flame stabilization.

The relatively high frequency of the TS current pulses also enabled us to study a ‘memory’ effect on the streamer-to-spark transition process and the breakdown mechanism. Decrease of N due to pre-heating and the accumulation of atomic oxygen could significantly suppress electron attachment frequency and thus explain no decrease of current after the streamer at frequencies above ~ 6 kHz in TS at the initial temperature $T_i = 300$ K. The memory effect influences the RS discharge as well. Several RS discharge parameters are functions of both the temperature and the frequency up to ~ 6 kHz. At higher frequencies, they depend only on the RS repetition frequency. Further research on the memory effect in self pulsing discharges is required to explain these findings in more detail. This should include improved chemical kinetic modeling and laser absorption and fluorescence diagnostic techniques focused on non-radiative species. The improved kinetic model must simulate the repetitive character of the studied discharges with the relaxation phase between current pulses. The diffusion processes should be also included at least during the relaxation phase.

Acknowledgments

Effort sponsored by the Slovak Research and Development Agency APVV-0134-12 and the French Ministry of Foreign Affairs under the Stefanik Franco-Slovak mobility program APVV SK-FR-0038-09 and the Slovak Grant Agency VEGA 1/0998/12.

References

- [1] Penetrante B and Schultheis S E 1993 *Non-Thermal Plasma Techniques for Pollution Control* (NATO Series vol 1) (New York: Springer)
- [2] Fridman A 2008 *Plasma Chemistry* (New York: Cambridge University)
- [3] Starikovskaia S M and Starikovskii A Y 2010 *Plasma assisted ignition and combustion Handbook on Combustion (Fundamentals and Safety vol 1)* (Weinheim: VCH Wiley)
- [4] Machala Z, Hensel K and Akishev Y 2012 *Plasma for Bio-Decontamination, Medicine and Food Security NATO Science for Peace and Security Series A Chemistry and Biology* (Heidelberg: Springer)
- [5] Kunhardt E E and Luessen L H 1983 *Electrical Breakdown and Discharges in Gases* NATO ASI Series, Part B *Macroscopic Processes and Discharges* vol 89b (New York: Springer)
- [6] Raizer Y P 1991 *Gas Discharge Physics* (New York: Springer)
- [7] Braithwaite N S J 2000 *Plasma Sources Sci. Technol.* **9** 517–27
- [8] Conrads H and Schmidt M 2000 *Plasma Sources Sci. Technol.* **9** 441–54
- [9] Efremov N M, Adamiak B Y, Blochin V I, Dadashev S J, Dmitriev K I, Gryaznova O P and Jusbashev V F 2000 *IEEE Trans. Plasma Sci.* **28** 238
- [10] Kogelschatz U 2003 *Plasma Chem. Plasma Proc.* **23** 1
- [11] Wagner H-E, Brandenburg K R, Sonnenfeld A, Michel P and Behnke J F 2003 *Vacuum* **71** 417
- [12] Mizuno A, Clements J S and Davis R H 1986 *IEEE Trans. Indust. Appl.* **22** 516–22
- [13] Lowke J J and Morrow R 1995 *IEEE Trans. Plasma Sci.* **23** 661–71
- [14] Penetrante B M, Bardsley J N and Hsiao M C 1997 *Japan. J. Appl. Phys.* **36** 5007–17
- [15] Masuda S and Nakao H 1990 *IEEE Trans. Indust. Appl.* **26** 374–83
- [16] Walsh J L, Shi J J and Kong M G 2006 *Appl. Phys. Lett.* **89** 161505
- [17] Pai D, Lacoste D A and Laux C O 2008 *IEEE Trans. Plasma Sci.* **36** 974–5
- [18] Bastien F and Marode E 1979 *J. Phys. D: Appl. Phys.* **12** 249
- [19] Machala Z, Morvová M, Marode E and Morva I 2000 *J. Phys. D: Appl. Phys.* **33** 3198
- [20] Machala Z, Marode E, Laux C O and Kruger C H 2004 *J. Adv. Oxid. Technol.* **7** 133
- [21] Yu L, Laux C O, Packan D M and Kruger C H 2002 *J. Appl. Phys.* **91** 2678
- [22] Staack D, Farouk B, Gutsol A and Fridman A 2005 *Plasma Sources Sci. Technol.* **14** 700
- [23] Akishev Y S, Aponin G I, Grushin M E, Karal'nik V B, Pan'kin M V, Petryakov A V and Trushkin N I 2008 Alternating nonsteady gas-discharge modes in an atmospheric-pressure air flow blown through a point-plane gap *Plasma Phys. Rep.* **34** 312–24
- [24] Akishev Y, Grushin M, Karalnik V, Petryakov A and Trushkin N 2010 *J. Phys. D: Appl. Phys.* **43** 215202
- [25] Marode E, Goldman A and Goldman M 1993 High pressure discharge as a trigger for pollution control *Non-Thermal Plasma Techniques for Pollution Control NATO ASI Series, Part A* (Berlin: Springer) pp 167–90
- [26] Hafez R, Samson S and Marode E 1995 A prevented spark reactor for pollutant control. Investigation of NO_x removal *12th Int. Symp. on Plasma Chemistry (Minneapolis, MN, USA, 21–25 August 1995)* pp 855–61
- [27] Marode E 2012 The prevented spark plasma in atmospheric air: from field to thermal equilibrium *Plasma for Environmental Issues* (Sofia: Artgraf)
- [28] Machala Z, Janda M, Hensel K, Jedlovský I, Leštinská L, Foltin V, Martišovič V and Morvová M 2007 *J. Mol. Spectrosc.* **243** 194
- [29] Janda M, Martišovič V and Machala Z 2011 *Plasma Sources Sci. Technol.* **20** 035015
- [30] Janda M, Machala Z, Niklová A and Martišovič V 2012 *Plasma Sources Sci. Technol.* **21** 045006
- [31] Machala Z, Jedlovský I, Chládeková L, Pongráč B, Giertl D, Janda M, Šikurová L and Polčič P 2009 *Eur. Phys. J. D* **54** 195
- [32] Janda M, Machala Z, Lacoste D A, Stancu G D and Laux C O 2012 Stabilization of a lean methane-air flame using transient spark discharge *13th Int. Symp. on High Pressure Low Temperature Plasma Chemistry (Kazimierz Dobny, Poland, 9–14 September 2012)* pp 185–9
- [33] Mitchell J B A 1990 *Phys. Rep.* **186** 215
- [34] Johnsen R 1993 *J. Chem. Phys.* **98** 5390
- [35] Capitelli M, Ferreira C M, Gordiets B F and Osipov A I 2000 *Plasma Kinetics in Atmospheric Gases Springer Series on Atomic, Optical and Plasma Physics* (New York: Springer)

- [36] Allen N L and Ghaffar A 1995 *J. Phys. D: Appl. Phys.* **28** 338
- [37] Pai D Z, Lacoste D A and Laux C O 2010 *J. Appl. Phys.* **107** 093303
- [38] Yin Z and Adamovich I V 2011 Ignition delay and time-resolved temperature measurements in nanosecond pulse hydrogen-air and ethylene-air plasmas at elevated initial temperatures *49th AIAA Aerospace Sciences Meeting (Orlando, Florida, 4–7 January 2011)* pp 2011–906
- [39] Peek F W Jr 1929 *Phenomena in High Voltage Engineering* (New York: McGraw-Hill)
- [40] Llewellyn-Jones F 1966 *Ionization and Breakdown in Gases* (London: Methuen)
- [41] Meek J M and Craggs J D 1978 *Electrical Breakdown of Gases* (New York: Wiley)
- [42] Marode E 1975 *J. Appl. Phys.* **46** 2005–16
- [43] Lowke J J 1992 *J. Phys. D: Appl. Phys.* **25** 202
- [44] Morrow R and Lowke J J 1997 *J. Phys. D: Appl. Phys.* **30** 614–27
- [45] Kulikovskiy A A 1998 *IEEE Trans. Plasma Sci.* **26** 1339–46
- [46] Larsson A 1998 *J. Phys. D: Appl. Phys.* **31** 1100–8
- [47] Naidis G V 1999 *J. Phys. D: Appl. Phys.* **32** 2649–54
- [48] Aleksandrov N L and Bazelyan E M 1999 *Plasma Sources Sci. Technol.* **8** 285–94
- [49] Kulikovskiy A A 2001 *IEEE Trans. Plasma Sci.* **29** 313–7
- [50] Bourdon A, Bonaventura Z and Celestin S 2010 *Plasma Sources Sci. Technol.* **19** 034012
- [51] Rusterholtz D L, Lacoste D A, Stancu G D, Pai D Z and Laux C O 2013 Ultrafast heating and oxygen dissociation in atmospheric pressure air by nanosecond repetitively pulsed discharges *J. Phys. D: Appl. Phys.* **46** 464010
- [52] Laux C O, Spence T G, Kruger C H and Zare R N 2003 *Plasma Sources Sci. Technol.* **12** 125
- [53] Derakhshesh M, Abedi J and Omidyeganeh M 2009 Modeling of hazardous air pollutant removal in the pulsed corona discharge *Phys. Lett. A* **373** 1051–7
- [54] Kacem S et al 2012 Full multi grid method for electric field computation in point-to-plane streamer discharge in air at atmospheric pressure *J. Comput. Phys.* **231** 251–61
- [55] Pancheshnyi S, Eismann B, Hagelaar G J M and Pitchford L C 2008 Computer code *zplaskin* *11th Int. Symp. on High Pressure, Low Temperature Plasma Chemistry (Oleron Island, France 7–12 September 2008)* www.zplaskin.laplace.univ-tlse.fr
- [56] Flitti A and Pancheshnyi S 2009 Gas heating in fast pulsed discharges in N₂–O₂ mixtures *Eur. Phys. J. Appl. Phys.* **45** 21001
- [57] Phelps database 2014 Retrieved on March 13 www.lxcat.net
- [58] Phelps A V and Pitchford L C 1985 *Phys. Rev. A* **31** 2932–49
- [59] Akishev Y S, Aponin G I, Grushin M E, Karal'nik V B, Monich A E, Pan'kin M V and Trushkin N I 2007 Development of a spark sustained by charging the stray capacitance of the external circuit in atmospheric-pressure nitrogen *Plasma Phys. Rep.* **33** 584–601
- [60] Marode E, Bastien F and Bakker M 1979 *J. Appl. Phys.* **50** 141–6
- [61] Xu D A, Lacoste D A, Rusterholtz D L, Elias P-Q, Stancu G D and Laux C O 2011 Experimental study of the hydrodynamic expansion following a nanosecond repetitively pulsed discharge in air *Appl. Phys. Lett.* **99** 121502
- [62] Xu D A, Shneider M N, Lacoste D A and Laux C O 2014 Thermal and hydrodynamic effects of nanosecond discharges in atmospheric pressure air *J. Phys. D: Appl. Phys.* **47** 235202
- [63] Akishev Y S, Aponin G I, Karal'nik V B, Monich A E and Trushkin N I 2004 Spatiotemporal evolution of the current and the integral and spectral emission characteristics of a negative corona in nitrogen during its transformation into a spark *Plasma Phys. Rep.* **30** 971–82
- [64] Sigmond S R 1984 *J. Appl. Phys.* **56** 1355
- [65] Bastien F and Marode E 1985 *J. Phys. D: Appl. Phys.* **18** 377
- [66] Marode E, Djermoune D, Dessante P, Deniset C, Segur P, Bastien F, Bourdon A and Laux C 2009 *Plasma Phys. Control. Fusion* **51** 124002
- [67] Janda M, Martišovič V, Hensel K, Dvonč L and Machala Z 2014 *Plasma Sources Sci. Technol.* **23** 065016
- [68] Loeb L B 1965 *Electrical Coronas* (Berkeley: University of California)
- [69] Stancu G D, Kaddouri F, Lacoste D A and Laux C O 2010 Atmospheric pressure plasma diagnostics by OES, CRDS and TALIF *J. Phys. D: Appl. Phys.* **43** 124002
- [70] Naidis G V 2009 *Eur. Phys. J. Appl. Phys.* **47** 22803
- [71] Janda M, Martišovič V, Hensel K, Dvonč L and Machala Z 2013 Time-resolved electrical and optical study of transient spark *16th Int. Conf. on Plasma Physics and Applications (Bucharest-Magurele, Romania 20–25 June 2013)* p 89